MRS Advances

Characterizing the Pressure Response of Microstructured Materials for Soft Optical Skins

Authors: Michael Portaro, Rio Brittany, Cindy Harnett

Affiliations: University of Louisville Department of Electrical and Computer Engineering

Abstract: Soft optical pressure-mapping elastomeric skins are an intrinsically stretchable and deformable platform to give robots a human-like tactile sense of their environment. In this work, we investigate how the microstructure of an elastomer layer controls its light transmission as a function of pressure. Under pressure, voids in a soft, optically-transmissive material will preferentially compress, influencing the tactile feel of the layer and increasing its solid contact area, allowing more light to escape at the pressure location. To study this concept, we made a microtextured silicone sheet and measured its optical transmission vs. incidence angle as a function of pressure. Increasing pressure on the sample monotonically increases the amount of light escaping the glass at the elastomer interface up to a plateau around 14 kPa. Such pressure-responsive microstructured layers will decouple the optical and mechanical requirements for waveguide materials used in soft optics-based sensing skins.

INTRODUCTION:

In optical pressure mapping skins like those shown in Figure 1, where contact between two optical waveguides allows light to cross from one to the other, there are two measurements: locating the pressure source and determining the pressure amplitude. For the location task, a specific contact junction can be identified by scanning sources and detectors (Fig. 1a,b), or by measuring the flight time of an optical pulse in a layered waveguide where a low refractive index interlayer has openings for the waveguides to make contact under pressure (Fig. 1c,d). For the pressure measurement task, some pressure amplitude information comes from the light intensity, because higher pressures generally lead to increased contact

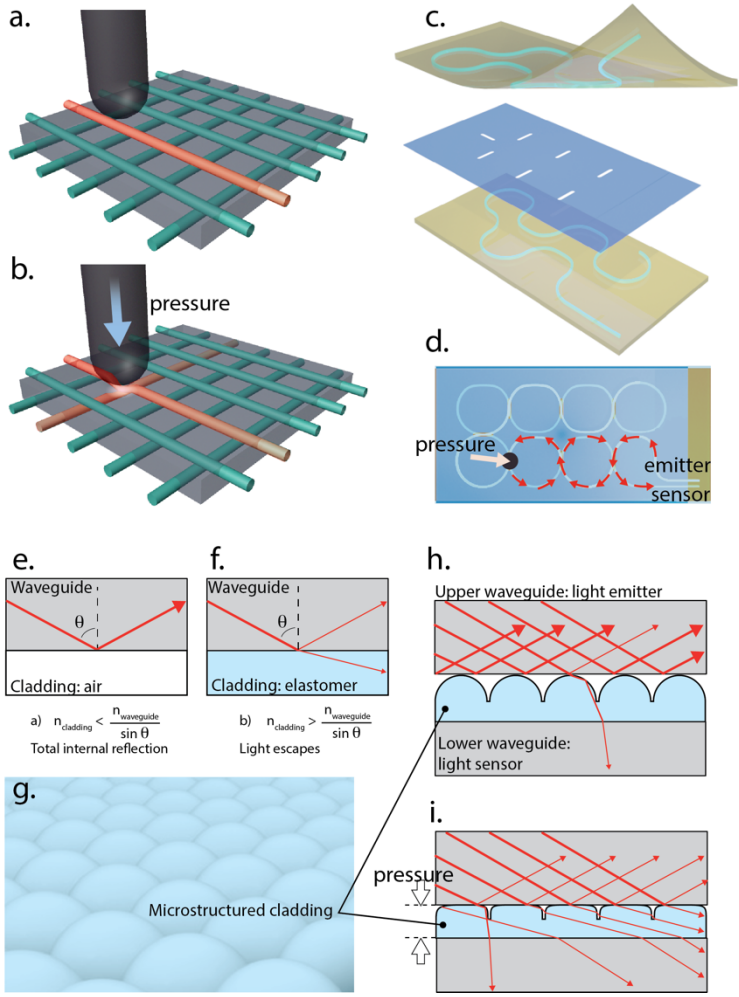

Fig. 1 a. Optical fiber grid with a lit fiber, b. Pressure causes inter-fiber coupling, c. Two-fiber system with a low refractive index interlayer that allows a sensor fiber and an emitter fiber to make contact at openings, d. Top view of two-fiber system showing how path length depends on location for a time-of-flight pressure mapping scheme, e. Total internal reflection at a waveguide-air interface, f. Partial internal reflection for the same angle at a waveguide-elastomer interface, g. Schematic of a microstructured cladding, h. Microstructured cladding stops most inter-fiber coupling at light pressure, i. At high pressure, the microstructures flatten and more light crosses from the emitter fiber to the sensor fiber

area between waveguide surfaces and more cross-coupling. However, the relationship between pressure and transmitted intensity is highly nonlinear. The transmitted light intensity depends on the fibers' optical and mechanical properties, and generally requires the fibers to be soft in order for human-generated forces to achieve a large range of interfacial contact areas. The goal of this work is to decouple the optical and mechanical demands with a pressure sensitive interlayer having tunable mechanical properties, and characterize its performance for device simulations and new device designs. The interlayer still needs to be optically transmissive, but not over long path lengths like the optical

waveguides in the upper and lower layers. Meanwhile, the optical waveguide layers need not be soft.

For a given core material, optical confinement in a core-clad structure is stronger for lower-index claddings, meaning rays with steeper incidence angles are totally reflected inside the core at the cladding interface. Fig. 1e and Fig. 1f show how contact with an elastomer (in this paper, a silicone with refractive index RI= 1.41) instead of air (RI =1) enables light to escape the waveguide (RI = 1.5, for example glass or soft urethane) at shallower angles than allowed with air. In most applications, an optical waveguide cladding is a solid material. However, in this work, the cladding is a molded structure made by casting a liquid-cure elastomer on a microstructured substrate (Fig. 1g). With this microstructure, pressure is expected to increase the fractional contact area of the elastomer with the waveguide core. For multimode waveguides such as the ~1 mm diameter, < 1 m long channels used in soft optical skins, light impinges on the core-cladding interface over a wide range of angles. If the unguided modes have not yet been lost to attenuation, as is the case for short waveguides, incidence angles can even be steeper than the total internal reflection angle. As shown in Fig. 1h and Fig. 1i, increasing pressure is expected to increase the intensity of light escaping the waveguide when the transmitted intensity is averaged over a region that samples several microcontacts.

Background

Researchers have long sought to do pressure mapping of human hand scale forces (sub 20 N) in the presence of interference from electromagnetic signals and with multi-touch capability. Free-space optical source and detector grids were one of the earliest touch-mapping technologies for human-computer interaction, appearing in the PLATO IV computer in 1972 [1]. These and subsequent edge-lit touchscreens could map human-generated touch through optical scattering, but aside from niche applications in large format and outdoor displays, electronic touchscreens dominated for cost and miniaturization reasons. Waveguides greatly simplified manufacturing, shrinking the interface circuit from the entire display edge down to two corners of the screen [2] for a lower-cost implementation. Because these touch-mapping methods lack tactile feedback and the ability to measure pressure amplitude, researchers also looked to soft materials that undergo large deformations when human-scale forces are applied. An early example of pressure amplitude sensing with a soft optical waveguide cited its ability to measure forces without electromagnetic interference [3], but did not map the force location. Optically responsive soft materials that change molecular orientation under stress have been deployed to measure strain in soft objects [4], to detect slipping objects in a grasping application [5], and as tactile sensors for robot hands [6]. Elastomeric “feelers” resembling the features in Fig. 1g have previously been investigated for optical pressure mapping [7]. These conical bumps collapse onto a glass or acrylic backplate under pressure, reflecting light in a pattern that forms an image of the pressure map. In contrast with imaging-based approaches, we aim to collect the averaged intensity into a waveguide for the non-imaging pressure mapping methods of Fig. 1 a-d in waveguiding skins that can be thin, nonplanar, and embedded in opaque layers. Others have used soft waveguides to achieve simultaneous pressure amplitude and location by threading previously developed elastomeric optical fibers [8] through three-dimensional (3D) paths in highly deformable printed scaffolds [9], then monitoring light transmission between waveguide pairs during object deformation. Although in this work we are considering a laminar optical skin, our microstructured interlayer might also be applied as a cladding to control inter-fiber coupling with these 3D

applications. In the rest of this manuscript we describe how the interlayer is fabricated and characterized, then show its optical response over a range of 0 to 2 PSI (0-14 kPa).

MATERIALS AND METHODS

Molding a microstructured optical interlayer

To make a microstructured optical interlayer, we obtained lenticular polycarbonate sheets (Rowlux Illusion Lenticular Films, ePlastics.com) with hemispheres in a hexagonal array having center-to-center spacing of 250 microns. Mold-making silicone (MoldStar 20T, Smooth-On, Inc.) was poured on the lenticular sheets and cured overnight to produce a silicone mold with cups instead of spheres. The mold was immersed in a 10:1 (volume) mineral spirits:petroleum jelly mold release solution for 1 minute, air dried, then covered with soft (Shore hardness 15A), optically clear liquid-cure silicone (Solaris, Smooth-On, Inc). The Solaris silicone was cured overnight, then peeled from the mold, forming an elastomeric replica of the lenticular film.

Measuring optical transmission as a function of angle and pressure

To characterize samples over a range of incidence angles and pressures, we developed a pressure refractometer from optomechanical parts, 3D printed parts and a load cell. It measures optical transmission through a sample under a range of normal forces.

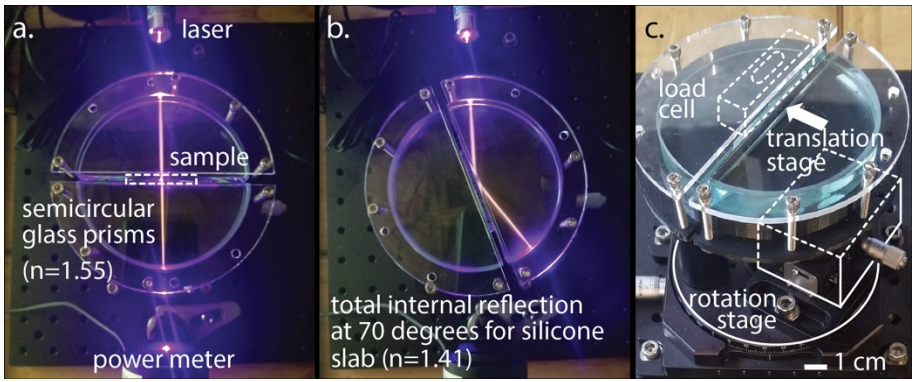

Fig. 2 Method for measuring optical transmission as a function of angle and pressure, illustrated with a 405 nm laser pointer and a silicone sample. a. Sample between two semicircular glass prisms. b. Rotating to various angles with respect to the laser and power meter. c. Pressure is applied with a translation stage and measured with a 5 kg load cell, each anchored to the rotation stage and each supporting one prism.

The power meter was a silicon photodiode with integrating sphere (PM16-140, ThorLabs, Inc). The load cell (TAL220B, SparkFun Electronics, Inc) was calibrated by turning the stage sideways and putting lab calibration weights on it while collecting data from a HX711 load cell amplifier (SEN-13879, SparkFun Electronics, Inc). The instrument can accommodate sample thicknesses up to 5 mm.

Measuring contact area as a function of pressure

To understand how the microstructures deform in response to pressure, a USB microscope camera was aimed at the sample through the side of the semicircular glass prism near the power meter, while the sample was compressed and the pressure was measured. Contact areas appeared dark because more of the incident light from the USB microscope source was able to escape to the opposite glass prism through the contact, compared to areas where air was present. The USB microscope images were thresholded and a particle analysis routine [10] was used to calculate the percentage of the region making contact with the elastomer. Images were collected for a range of pressures obtained by manually adjusting the translation stage and reading the load cell value.

RESULTS

Under pressure, the microstructured silicone layer increased its contact area with the surface as illustrated schematically in Fig. 1i. The microscope images in Fig. 3a and 3b show the appearance of dark contact regions, and Fig. 3c shows their relative size compared to the laser beam, which covers approximately 200 contacts.

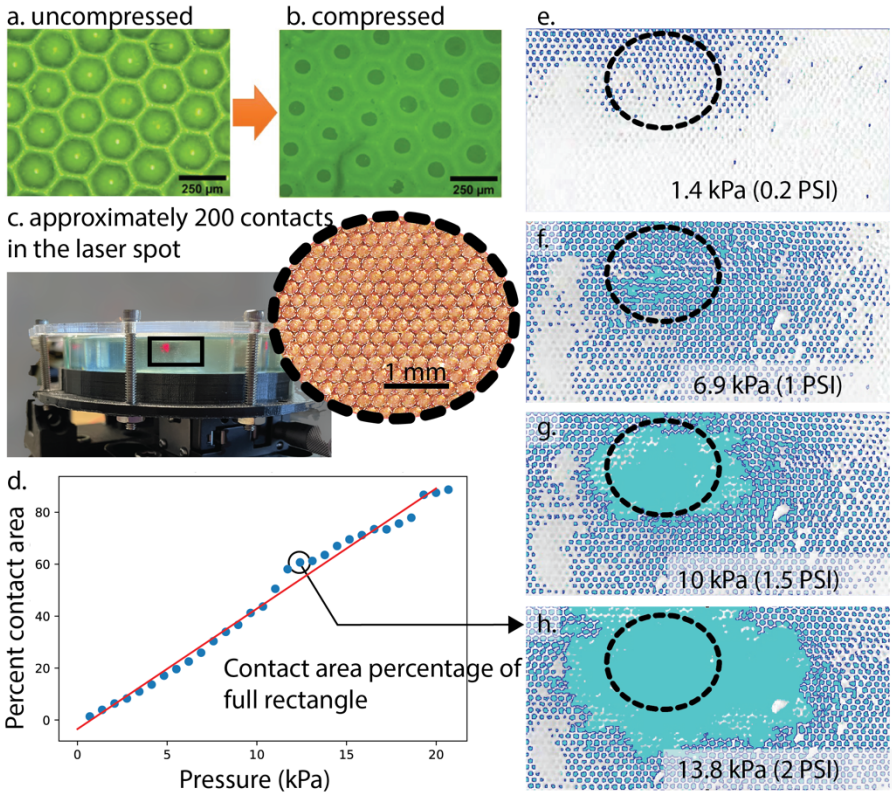

Fig. 3 a. Microscope view of uncompressed and b. compressed layer showing dark appearance of contact areas, c. The laser spot of the pressure refractometer samples approximately 200 contacts, d. Image analysis of contacts at increasing pressures (e-h)

Neighboring contacts collapsed together under increasing pressure. At approximately 2 PSI (14 kPa), the contacts merged forming a large (~10 mm) connected region near the center of the sample (Fig. 3h) and covering the laser spot. This non-uniformity was most likely caused by small variations in the sample thickness. At 3 PSI (20 kPa), shown on the far right of the plot in Fig. 3d, nearly 90% of the rectangle imaged in Fig. 3 e-h had merged into the contact region. The percent contact area increase was nearly linear (Fig. 3d) up until this pressure range, beyond which the microstructured interlayer behaved like a solid silicone layer.

The rotation stage was moved in five-degree increments, and optical transmission-vs-pressure data were collected at each angle by moving the translation stage. These results are shown in Figure 4a, along with calculated transmission *vs.* angle for "samples" of air or solid silicone (Fig. 4b). For an intermediate angle (55 degrees) betweeen the glass-air critical angle of 45 degrees and the glass-silicone critical angle of 69 degrees, Fig. 4c shows transmitted intensity *vs.* pressure.

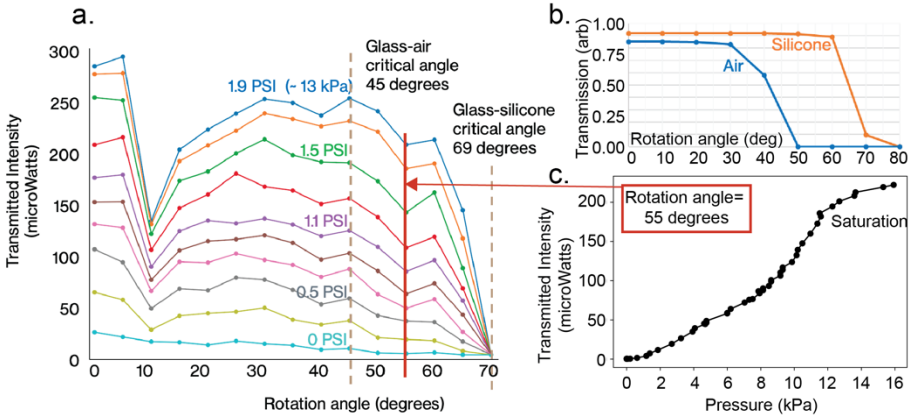

Fig. 4 a. Transmitted intensity for all rotation angles and pressures at 633 nm, b. Calculated transmission *vs.* angle for both of the constituent materials in the microstructure, c. Transmitted intensity *vs*. pressure for a fixed angle (55 degrees).

The drop in intensity at 10 degrees was seen repeatedly and may be a corner cube reflector effect originating between the hemispheres. In a waveguide application, however, the majority of incidence angles are expected to be above the core-cladding critical angle (here, for an unclad glass waveguide, 45 degrees) because unguided rays with smaller incidence angles are lost from the device, while rays above the glass-silicone critical angle (here 69 degrees) stay internally reflected. Therefore, the angles of interest for most applications of this interlayer are between 45 and 69 degrees. Fig. 4c shows transmitted intensity *vs.* pressure for one such intermediate angle. Intensity *vs*. pressure plots for these intermediate angles showed monotonically increasing transmission until a plateau around 14 kPa (2 PSI) where the contacts in the laser spot region had mostly merged (Fig. 3h). Below this plateau pressure, the interlayer has successfully transformed increasing pressure into an increasing optical transmission signal using a soft microstructured material.

CONCLUSIONS

This manuscript has described a microstructured interlayer with collapsing voids for controlling optical transmission as a function of pressure. Whether the voids are randomly

distributed or deterministically placed by molding, such surfaces take on new optical and mechanical properties thanks to their geometry. Changing the designs of the micromachined features might allow one to further tune the pressure response, for example buckling at a threshold pressure or responding to shear forces. The work here was performed on liquid cured elastomers, but porogens incorporated into 3D printable filaments such as clear thermoplastic urethane could enable additive manufacturing of microstructured optical surfaces without high-resolution printing or molding. To maximize transmission along waveguide sections where pressure is not applied, both sides of the interlayer should have a microstructure for a low averaged index and strong waveguiding. This type of structure could be accomplished by two-sided molding, by placing two interlayers back-to-back, or by the above mentioned porous materials. Developments in this area will lead to all-polymer surfaces that measure and map deformation on a force scale controlled by the interlayer material's design.

ACKNOWLEDGMENTS

Support was received from NSF awards 1849213 and 1935324.

DATA

The datasets generated during and/or analysed during the current study are available from the corresponding author on reasonable request.

CONFLICT OF INTEREST

On behalf of all authors, the corresponding author states that there is no conflict of interest.

References:

[1] D. V. Meller, "Using PLATO IV" 1975. [Online]. Available: https://eric.ed.gov/?id=ED124144.

[2] H. C. Pedersen, M. L. Jakobsen, S. G. Hanson, M. Mosgaard, T. Iversen, and J. Korsgaard, "Optical touch screen based on waveguide sensing," *Appl. Phys. Lett.*, vol. 99, no. 6, p. 061102, Aug. 2011.

[3] Y. Shibata, A. Nishimura, S.-I. Niwa, Y. Osawa, and T. Uemiya, "Optical sensor," 4750796, 14-Jun-1988.

[4] D. Mistry *et al.*, "Isotropic Liquid Crystal Elastomers as Exceptional Photoelastic Strain Sensors," *Macromolecules*, vol. 53, no. 10, pp. 3709–3718, May 2020.

[5] V. N. Dubey and R. M. Crowder, "A dynamic tactile sensor on photoelastic effect," *Sens. Actuators A Phys.*, vol. 128, no. 2, pp. 217–224, Apr. 2006.

[6] M. Mitsuzuka *et al.*, “Relationship between Photoelasticity of Polyurethane and Dielectric Anisotropy of Diisocyanate, and Application of High-Photoelasticity Polyurethane to Tactile Sensor for Robot Hands,” *Polymers* , vol. 13, no. 1, p. 143, Dec. 2020.

[7] M. Ohka, J. Takata, H. Kobayashi, H. Suzuki, N. Morisawa, and H. Yussof, “Optical three-axis tactile sensor for robotic fingers,” *Sensors: Focus Tactile Force Stress Sensing; InTech: Rijeka, Croatia*, pp. 103–122, 2008.

[8] C. K. Harnett, H. Zhao, and R. F. Shepherd, “Stretchable Optical Fibers: Threads for Strain-Sensitive Textiles,” *Adv. Mater.*, 2017.

[9] P. A. Xu, A. K. Mishra, H. Bai, C. A. Aubin, L. Zullo, and R. F. Shepherd, “Optical lace for synthetic afferent neural networks,” *Science Robotics*, vol. 4, no. 34, p. eaaw6304, 2019.

[10] J. Schindelin *et al.*, “Fiji: an open-source platform for biological-image analysis,” *Nat. Methods*, vol. 9, no. 7, pp. 676–682, Jun. 2012.